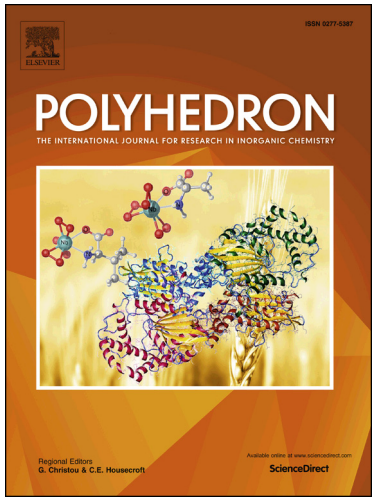

Copper mesoporous materials as highly efficient recyclable catalysts for the reduction of 4-nitrophenol in aqueous media

Sofía Schlichter, Mariana Rocha, Andreia F. Peixoto, João Pires, Cristina Freire, Mariana Alvarez

PII: S0277-5387(18)30214-6
DOI: https://doi.org/10.1016/j.poly.2018.04.037
Reference: POLY 13139

To appear in: *Polyhedron*

Received Date: 31 January 2018
Accepted Date: 23 April 2018

Please cite this article as: S. Schlichter, M. Rocha, A.F. Peixoto, J. Pires, C. Freire, M. Alvarez, Copper mesoporous materials as highly efficient recyclable catalysts for the reduction of 4-nitrophenol in aqueous media, *Polyhedron* (2018), doi: https://doi.org/10.1016/j.poly.2018.04.037

Copper mesoporous materials as highly efficient recyclable catalysts for the reduction of 4-nitrophenol in aqueous media

Sofía Schlichter[1], Mariana Rocha[2], Andreia F. Peixoto[2*], João Pires[3], Cristina Freire[2*], Mariana Alvarez[1*]

[1]*INQUISUR, Departamento de Química, Universidad Nacional del Sur, Av. Alem 1253, 8000, Bahía Blanca, Argentina.*

[2]*REQUIMTE/LAQV, Departamento de Química e Bioquímica, Faculdade de Ciências, Universidade do Porto, Rua do Campo Alegre s/n, 4169-007 Porto, Portugal.*

[3]*Departamento de Química e Bioquímica, CQB and CQE, Faculdade de Ciências, Universidade de Lisboa, Ed. C8, Campo Grande, 1749-016 Lisboa, Portugal.*

**Correspondence e-mail:* andreia.peixoto@fc.up.pt, acfreire@fc.up.pt, alvarezm@criba.edu.ar

ABSTRACT

Two mesoporous-based catalysts with different nominal copper loads (10 and 24 % w/w) were prepared from impregnation of the MCM-41 support with copper acetylacetonate: Cu/MCM-41-10 and Cu/MCM-41-24, respectively. Samples with a metallic charge similar to the nominal content were obtained and the mesoporous structure was retained after the impregnation. X-ray diffractograms evidenced the presence of CuO in the catalyst with the higher metal loading. The catalytic reduction of 4-nitrophenol (4-NP) to 4-aminophenol (4-AP) in aqueous medium, with an excess of $NaBH_4$, was chosen as a model reaction to evaluate the catalytic activity of the Cu/MCM-41-10 and Cu/MCM-41-24 catalysts. The 4-NP concentrations at prefixed intervals were monitored using UV–Visible spectroscopy. The Cu-based catalysts led to almost 100% reduction of 4-NP to 4-AP, with the reaction time of 30 and 50 sec, for Cu/MCM-41-10 and Cu/MCM-41-24 respectively. The reaction follows a pseudo-first order law, with a rate constant of 0.374 and 0.109 s^{-1} for Cu/MCM-41-10 and Cu/MCM-41-24, respectively. Both catalysts were stable and could be reused up to ten times in consecutive runs without any treatment between the cycles. The catalytic activity was retained without loss of efficiency, indicating the high stability of the MCM-41 based catalysts under the reaction conditions.

Keywords: Copper catalysts, MCM-41, 4-Nitrophenol reduction, $NaBH_4$.

1. INTRODUCTION

4-Nitrophenol (4-NP) is a common pollutant of the nitroarene group, typically produced as a by-product in the pharmaceutical, agrochemical, textile and dye chemical industries [1,2]. Consequently, it is inevitably released into the environment as an industrial effluent, contaminating both surface and groundwater [3]. The main problems are that it can be carcinogenic and genotoxic, affecting human and wildlife [4,5]. To deal with this problem, different treatments, like adsorption, electrochemical and microbial degradation, are employed. However, degradation of 4-NP to non-dangerous product is difficult because of its high stability and low solubility in water [6].

On the other hand, 4-NP selective reduction has acquired significant importance since the reaction product is 4-aminophenol (4-AP), which is a main industrial intermediate for manufacturing analgesic and antipyretic drugs, anticorrosion lubricants and hair dyeing agents [7,8]. Thus, the reduction of 4-NP becomes interesting from both an environmental and industrial point of view. Therefore, the design of an efficient low cost and recoverable catalyst for the remediation of contaminated sources with this toxic organic compound by reduction to a less toxic amine, is now a great challenge.

The common and most efficient way for the reduction of 4-NP in aqueous media is employing $NaBH_4$ as a reductant together with a metal catalyst. Gold is by far the most extensively studied catalyst for this reaction [9,10], followed by other noble metals such as palladium and platinum [11,12]. However, there is a demand to replace these costly and scarce noble metals by non-precious metals based on Ni [13], Zn [14] and Co [15] for use in this type of nitroarene reduction.

Among them, copper nanoparticles (Co NPs) are of high interest due to their high-stability, environmental friendly nature, low-cost and the fact they can be applied as catalysts in nitroarene reductions, achieving great conversions under mild conditions,

even at ambient or lower temperatures [16,17,18]. Nevertheless, copper NPs suffer from certain disadvantages such as metal aggregation and precipitation which cause catalyst decomposition and a considerable loss of activity, moreover they are difficult to reuse after reactions which leads to a loss of metal and contaminations [19,20]. Hence, the use of heterogeneous copper catalysts is often advantageous from the perspective of process development due to their easy handling, stability, effortless recovery and recycling [16,19,21,22,23,24,25]; the selection of the support is a crucial point to achieve these advantages. Cu NPs have been applied in nitroarene reduction immobilized onto various supports, including graphene [23], cellulose nanofibers [16] and magnetic carbon materials [26]. Mesoporous oxides are excellent examples of a good support, combining a high specific surface area with an ordered structure of wide pores and allowing a high concentration of active sites with free diffusion of reactants and products. Recently well-ordered mesoporous-silica has been used as a support for ruthenium nanoparticles for the highly selective reduction of functionalized nitroarenes.[27]

So far, to our knowledge, MCM-41 has never been previously used as a copper support to be applied in the reduction of 4-NP to 4-AP in aqueous media. In the present work, the mesoporous silicate MCM-41 was impregnated with copper acetylacetonate in order to obtain Cu-based catalysts with different copper loadings. Their catalytic performance in 4-NP reduction in terms of the rate constant and the induction period, as well as catalyst reusability, was discussed through a comparison with other Cu-catalysts.

2. MATERIALS AND METHODS

2.1. Support synthesis

All the reagents were analytical grade and were used as received without further purification. The hexagonal MCM-41 was synthesized following the specifications of Bore *et al.* (2006) [28]. For that, cetyltrimethyl ammonium bromide (CTAB) surfactant dissolved in water and sodium silicate (SiO_2 27%, NaOH 10%, H_2O 63%) was added to a batch reactor. The molar ratio of the precursor solution was $3.4SiO_2$:1CTAB:$286H_2O$. The pH was adjusted to 10 with 1 M HNO_3 and the mixture was kept in a water bath under static conditions for 8 h at 80 °C. After that, it was cooled down to room temperature. The solid was filtered under vacuum and washed several times with distilled water. The actual yield was 90 % with respect to the theoretical yield of precipitated silica. The total weight of silica (SiO_2) present in whole sodium silicate was taken as the theoretical yield, as it is stated in [26].

2.2. Catalysts synthesis

Samples were prepared by contacting a solution of copper acetylacetonate, $Cu(AcAc)_2$, in toluene with MCM-41 at 70 °C under continuous stirring for 24 h [18]. The target metal concentration was 10 or 24 wt%. Approximately 10 mL of solution and 1 g of MCM-41 were employed. In order to remove the surfactant, the material was dried at 70 °C for 4 h and calcined at 400 °C for 6 h (0.5 °C/min). The catalysts were named as Cu/MCM-41-X, where X indicates the nominal theoretical metal loading.

2.3. Catalyst characterization

The structural properties of the supports and the catalysts were determined by X-ray diffraction (XRD) at room temperature over the range 2θ = 2-70º with a Philips PW1710 BASED diffractometer (45 kV, 30 mA) using $CuK\alpha_1$ radiation (λ = 1.5406 Å) using a graphite monochromator and the Bragg-Brentano $\theta/2\theta$ configuration.

In order to obtain information on the morphological characteristics, the catalysts were subjected to Transmission Electron Microscopy (TEM) analysis. TEM micrographs were obtained on a JEOL 100X2 (Tokyo, Japan) apparatus. Samples for TEM were prepared by the solvent casting method on a Cu grid with a carbon support membrane.

Fourier transform infrared spectra (FTIR) were collected with a FTIR-NIR Thermo Scientific Nicolet iS50 spectrophotometer in the 400–4000 cm^{-1} range using a resolution of 4 cm^{-1} and 32 scans. The spectra of the samples were obtained in KBr pellets containing 1 wt% of sample.

The copper content was determined by acidic disgregation of the samples by atomic absorption spectroscopy (AAS) using a GBC Avanta Model B-932.

The textural properties of the catalysts were determined from nitrogen adsorption–desorption isotherm data at 77 K obtained in an automatic volumetric adsorption apparatus (Quantachrome 2200e). Prior to nitrogen adsorption, the samples were outgassed for 150 min at 423 K. The specific surface areas were calculated using the Brunauer, Emmett and Teller method (BET).

X-ray photoelectron spectroscopy (XPS) was performed at the Centro de Materiais da Universidade do Porto (CEMUP, Porto, Portugal) in a KRATOS AXIS Ultra HSA - VISION spectrometer using monochromatized Al Kα radiation (1486.6 eV) operating at 15 kV (90 W) in the FAT (Fixed Analyser Transmission) mode. The powdered samples were pressed into pellets for XPS studies. All binding energies (BE) were referenced to the C 1s line at 284.6 eV.

2.4. Catalytic reduction of 4-NP

The catalytic reduction of 4-NP to 4-AP was conducted at room temperature in a 3 mL quartz optical cell and monitored by spectral scans on an Agilent 8453 UV-Vis

spectrometer with a diode array detector in the range 250-550 nm. A stock solution of 4-NP (0.05 mmol/L) was employed for all experiments. For the kinetic study, 3 mL of this 4-NP solution was transferred to the UV-Vis cell followed by the addition of 5.4 mg of $NaBH_4$ (0.15 mmol). Upon $NaBH_4$ addition, the original absorption peak of 4-NP centered at 317 nm shifted to 400 nm due to the formation of the 4-nitrophenolate ion. The reaction only started after the addition of the catalyst. The solid catalyst (1 mg for Cu-MCM-41-10 or 3 mg for Cu-MCM-41-24) was added to the cuvette and the degradation reaction was controlled at 2 s intervals for Cu-MCM-41-10 and 5 s for Cu-MCM-41-24. The catalyst/4-NP/$NaBH_4$ mass ratio was 1/0.021/5.4 for Cu/MCM-41-10 and 3/0.021/5.4 for Cu-MCM-41-24. These reaction conditions were chosen based on previous literature work [10].

For the reusability test, a scaled-up experiment with 20 mg of catalyst was carried out in a round bottom flask under stirring at room temperature and maintaining the same catalyst/4-NP original ratio. Spectra were collected after 30 s of reaction by withdrawing 3 mL aliquots from the reaction medium. After each catalytic cycle, the solids were filtered and the catalyst was reused in a new experiment without any prior treatment. This procedure was repeated up to ten times and after that the material was washed with deionized water and dried for further characterization.

3. RESULTS AND DISCUSSION

3.1. Catalysts characterization

The XRD technique was used to confirm the mesoporous structure and evaluate support profile changes after metal incorporation. The diffractogram of the mesoporous support (Figure 1) showed a typical pattern for hexagonal mesoporous MCM-41 [29]. A strong (100) Bragg reflection centered at about $2\theta = 2.5°$ and minor peaks at $2\theta = 4.2$,

4.8 and 6.4º, attributed to (110), (200) and (210) diffractions respectively, were observed. These peaks are assigned to the MCM-41 structure with a two-dimensional hexagonal p6mm symmetry, demonstrating the high quality of the mesoporous packing [30].

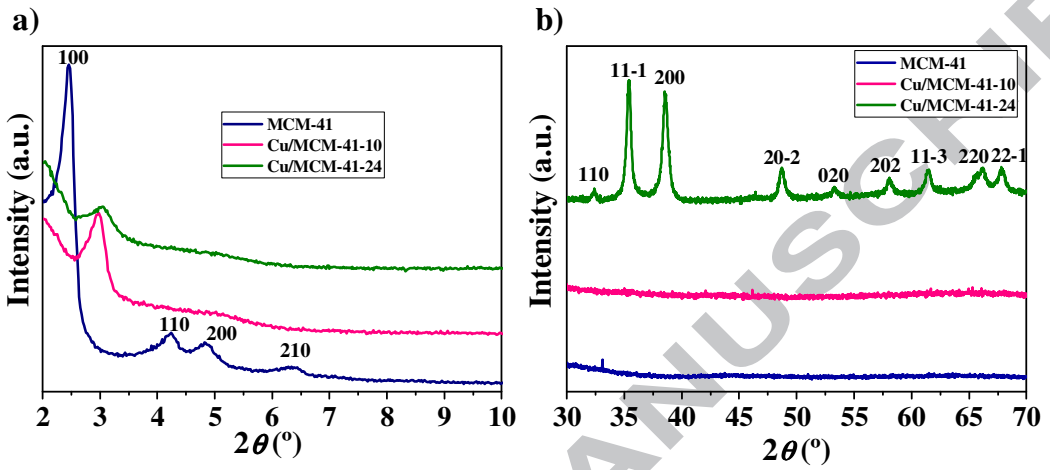

Figure 1. X-Ray diffractograms of the pristine MCM-41 material and after loading with two Cu amounts (10 and 24 wt%): a) low-angle and b) wide angle.

The unit cell parameter (a_0) was determined by equation 1, where d_{100} was estimated from the diffraction peak (100) by the Bragg's equation ($2d\sin\theta = \lambda$).

$$a_0 = \frac{2d_{100}}{\sqrt{3}} \qquad (1)$$

The unit cell obtained (4.15 nm) is comparable with the two-dimensional hexagonal pore structure of typical MCM-41 materials [31].

The Cu/MCM-41-24 metal-modified material lower angle diffractogram (Figure 1) showed the typical main peak of the MCM-41 parent material and the wide-angle additional diffraction peaks at 32.4, 35.5, 38.6, 48.7 53.3, 58.1, 61.4, 66.2 and 67.9º are assigned to (110), (11-1), (200), (20-2), (020), (202), (11-3), (220) and (22-1), respectively, corresponding to the lattice planes of monoclinic CuO (JCPDS Card No 41-0254) [18, 32]. The sample Cu/MCM-41-24 presented a mean size for the CuO

particles of 15 nm, as calculated by the Debye-Scherrer formula using the diffraction (200).

In the case of the Cu/MCM-41-10 catalyst, the XRD results showed no diffraction peaks of copper oxides. Nevertheless, it is possible that copper oxide would appear as highly dispersed nanoclusters with particle sizes lower than the detection limit of the XRD technique. After the Cu impregnation, a broadening and a shift to higher 2θ value for the (100) peak was observed, indicating a slight distortion of the long range hexagonal symmetry [33]. In fact, the calculated unit cell parameters (a_0) are smaller compared to pristine MCM-41; 3.42 and 3.35 nm for the samples Cu/MCM-41-10 and Cu/MCM-41-24, respectively.

Figure 2 shows the TEM images. The pristine MCM-41 exhibits a hexagonal array of channels (Figure 2a). After metal loading, the samples show a more agglomerated morphology, but the mesoporous order is retained (Figure 2b-c), which is in agreement with the XRD results.

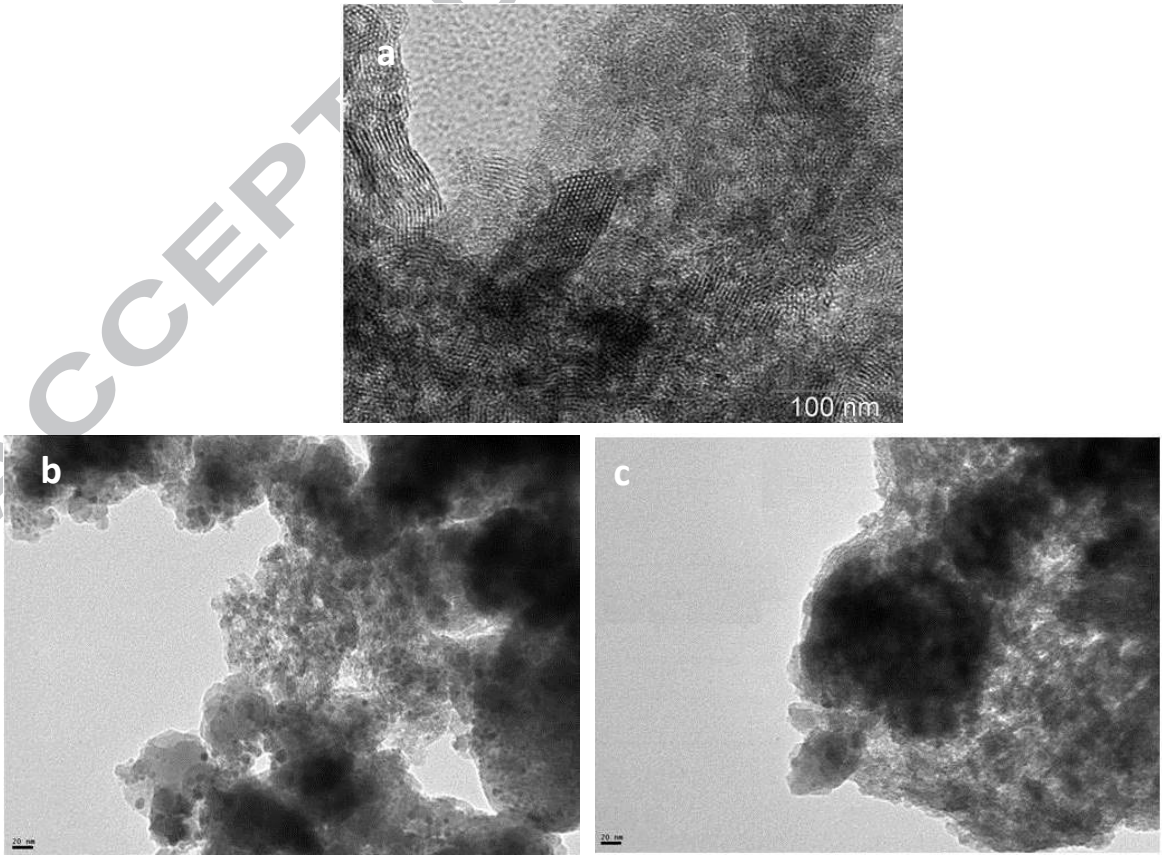

Figure 2. TEM images of (a) MCM-41, (b) Cu/MCM-41-10 and (c) Cu/MCM-41-24.

The FTIR spectra of the MCM-41 based-catalysts present the characteristic bands of the support structure (Figure 3). In all the cases, OH stretching vibration bands from silanol groups and adsorbed water appear in the 3370-3000 and 1650-1630 cm^{-1} regions. The vibration bands at 1080 (with a shoulder at 1230 cm^{-1}) and 462 cm^{-1} are assigned to Si-O-Si symmetric stretching and bending. The bands at 960 and 810 cm^{-1} are attributed to the symmetrical stretching vibration of the Si–OH and Si–O–Si groups, respectively. The Cu-containing catalysts also showed a band at ~960 cm^{-1} corresponding to Si–OH stretching vibration, although this was significantly larger than the parent MCM-41. This fact could be attributed to the replacement of Si–OH groups by Cu ligands, therefore justifying the difference between the bands of the Cu-modified catalysts and the parent material, evidencing the presence of copper ions in the MCM-41 mesoporous material [34,35].

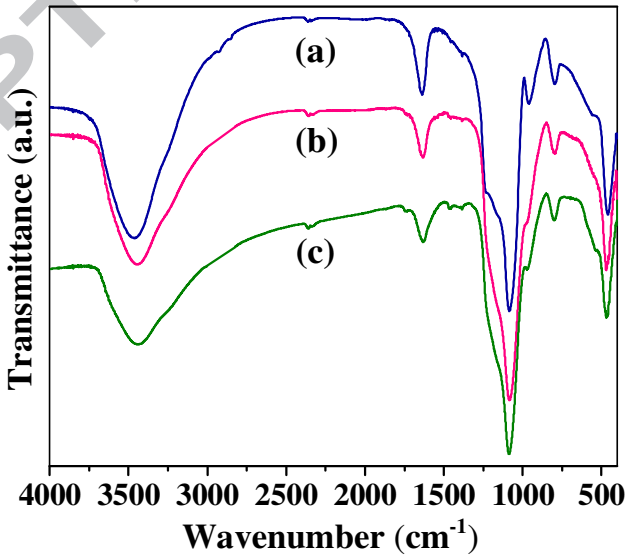

Figure 3. FT-IR spectra of (a) MCM-41, (b) Cu/MCM-41-10 and (c) Cu/MCM-41-24.

The copper content and its atomic percentage, obtained by AAS and XPS, are summarized in Table 1. Surface areas and pore diameters calculated from the N_2 isotherms are also included.

Table 1. Characterization of MCM-41 and Cu-modified MCM-41 by AAS, XPS and N_2 nitrogen sorption isotherm analyses.

Sample	Bulk Cu (wt%)[a]	Superficial Cu (%)[b]	Pore diameter (nm)[c]	BET area (m^2g^{-1})[c]
MCM-41	-	-	4.1	1007
Cu/MCM-41-10	5.8	3.0	2.6	547
Cu/MCM-41-24	18.0	3.6	-[d]	864

[a] Measured by AAS. [b] Calculated by XPS. [c]Calculated by N_2 isotherms. [d]Not determined

The total metal content given by AAS was slightly lower comparatively to the theoretical nominal loading in the case of the sample Cu/MCM-41-10. The efficiency of metal impregnation was 58 and 75% for the samples Cu/MCM-41-10 and Cu/MCM-41-24, respectively. This is also in good agreement with the previously reported XRD results, wherein characteristic CuO peaks appeared with the increment of nominal Cu loading. As can be seen, comparing the amounts of bulk Cu by AAS and the superficial Cu by XPS, most of the metal is on the surface of the material in the case of Cu/MCM-41-10; whereas for the sample Cu/MCM-41-24, taking into account the differences in Cu amounts, it is possible to predict that most of the Cu content was occluded in the material's porosity. From the results of the N_2 sorption analysis, it could be observed that quite large surface areas were obtained in the copper-modified materials. All the solids exhibited type IV isotherms with H1 hysteresis loops (IUPAC classification),[35] as could be expected for mesoporous materials. After the metal loading, there was a decrease of the BET area and pore diameter relatively to pristine MCM-41, due to the incorporation of the metal oxide thought the support surface and pores, which is in agreement with the FTIR results. Interestingly, a higher BET area for the sample

Cu/MCM-41-24 compared with Cu/MCM-41-10 was observed, indicating a better dispersion of Cu atoms in the material with the high Cu loading.

The oxidation state of copper on the catalyst surface was also investigated by XPS analysis. Two intense peaks at 935 and 955 eV along with two satellite peaks (938 - 946 eV) were attributed to Cu $2p_{3/2}$ and $2p_{1/2}$, which confirmed the existence of Cu^{2+} species (Figure 4) [36]. Literature studies showed that pure CuO presents a Cu 2p3/2 binding energy of 933.6 eV, thus the shift here observed toward higher energy could be indicative of a charge transfer from the copper(II) ion to the MCM-41 support. The $2p_{3/2}$ peak was deconvoluted into two different contributions that can be attributed to Cu^{2+} species at 935.4 eV and a small contribution of Cu^{0}/Cu^{+} species at 932.6 eV (Figure 4c and 4d) [37].

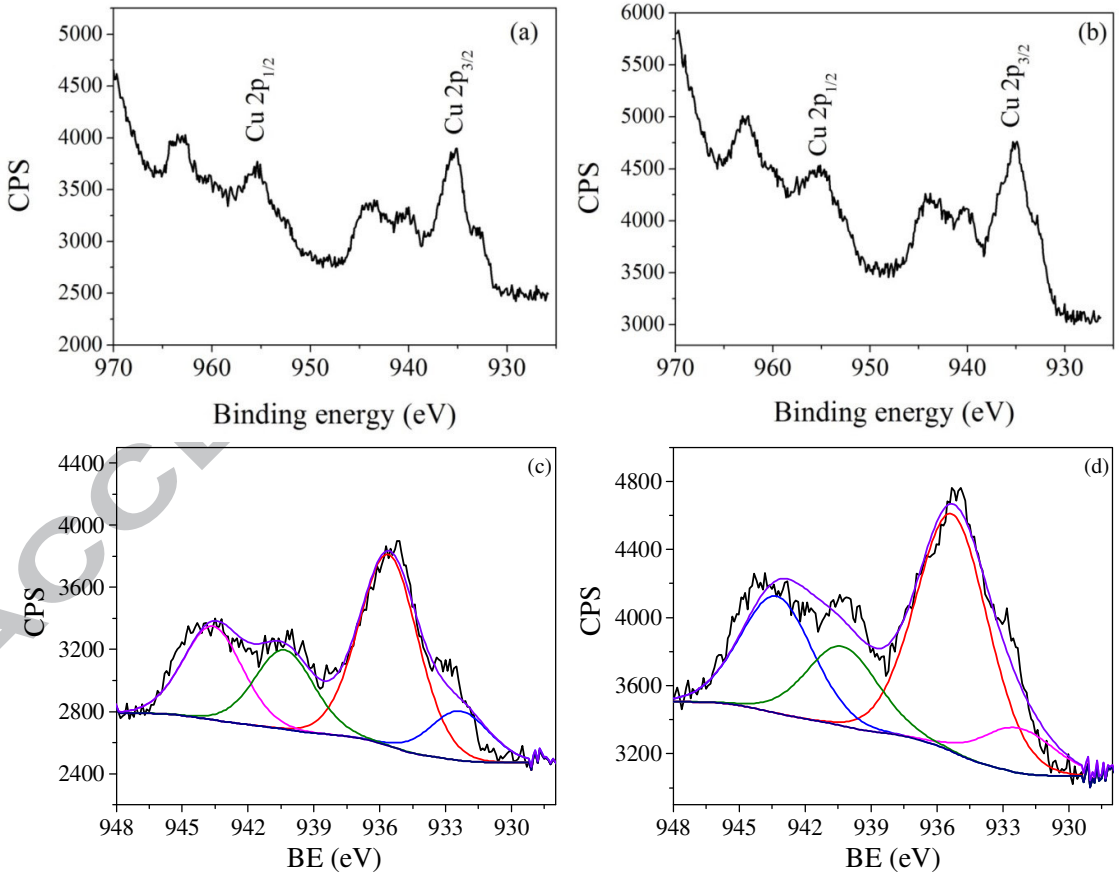

Figure 4. Cu2p high-resolution XPS spectra of (a) Cu/MCM-41-10 and (b) Cu/MCM-41-24. Deconvolution of Cu $2p_{3/2}$ high-resolution XPS spectra: (c) Cu/MCM-41-10 and (d) Cu/MCM-41-24. Pink line: Cu(I) species; red line: Cu(II) species and green and blue lines: shake up satellites, respectively.

These results confirm the presence of CuO in both Cu/MCM-41 samples, although there was no evidence of CuO characteristic peaks in the XRD diffractogram of Cu/MCM-41-10.

3.2. Catalytic degradation of 4-NP

The catalytic performance of the Cu catalysts for the reduction of 4-NP to 4-AP was tested with an excess amount of $NaBH_4$. The 4-NP degradation was monitored by UV–Vis spectroscopy, following the decrease of the electronic band absorbance at λ = 400 nm which corresponds to the presence of the nitrophenolate ion in basic media. A concomitant increase in the peak at about λ = 300 nm was observed, attributed to the reduced product, 4-aminophenol [38]. After the addition of $NaBH_4$ into the aqueous solution of 4-NP, the color of the solution changed from light yellow to dark yellow due to the 4-nitrophenolate ion formation. The color faded with time after the addition of Cu/MCM-41-10 (1 mg) or Cu/MCM-41-24 (3 mg). Both catalysts showed excellent catalytic activity in the 4-NP reduction, achieving a substrate maximum conversion of ca. 100 % within 30 and 50 s of reaction for Cu/MCM-41-10 and Cu/MCM-41-24, respectively (Figure 5 a-b). In the absence of catalyst, no color change was observed in this period, suggesting that $NaBH_4$ cannot reduce 4-nitrophenolate ions by itself.

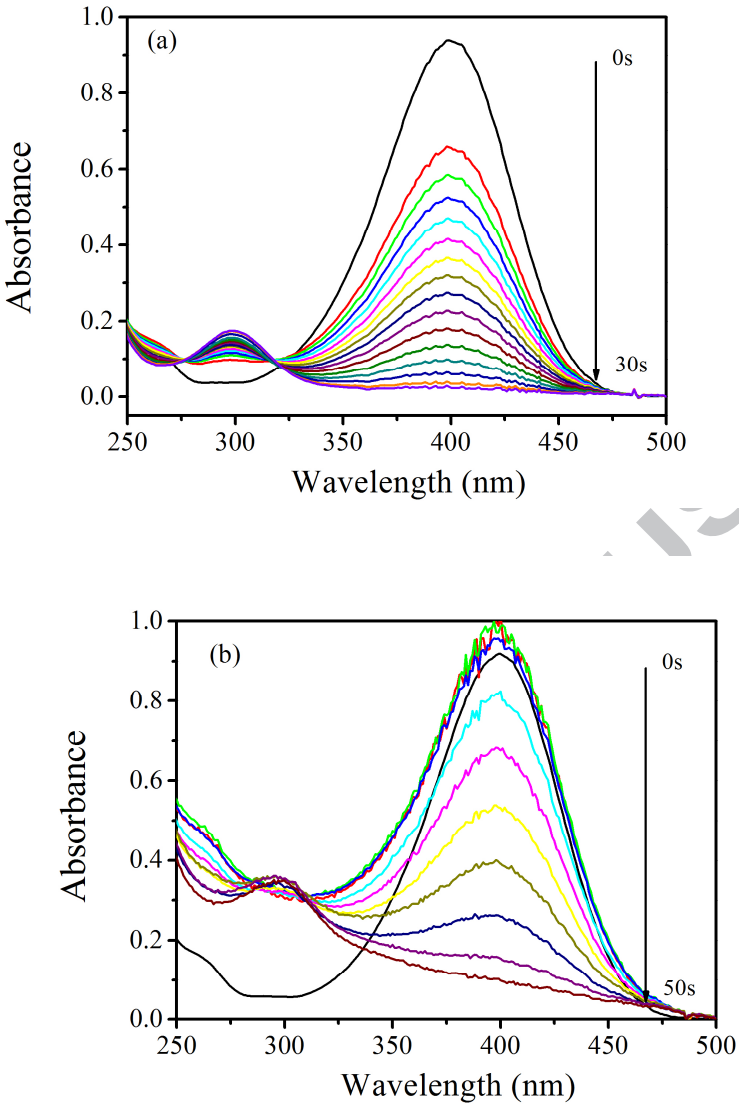

Figure 5. Time-dependent UV-visible absorption spectra for the reduction of 4-NP catalyzed by (a) Cu-MCM-41-10 and (b) Cu-MCM-41-24.

The catalytic reaction mechanism can be explained in terms of the Langmuir-Hinshelwood model [39]. This model states that the borohydride ions react with the catalyst surface and transfer hydrogen atoms to its surface. Simultaneously, the 4-NP molecules adsorb at the CuO NPs surface. Assuming that both the steps for diffusion of 4-NP and the CuO-NPs adsorption-desorption are fast, the reduction of 4-NP adsorbed by the surface-hydrogen species is the rate-determining step. The final step of the

catalytic cycle is the 4-AP desorption, which is fast and does not count in the kinetic equation. [40] A scheme of this model is presented in Figure 6.

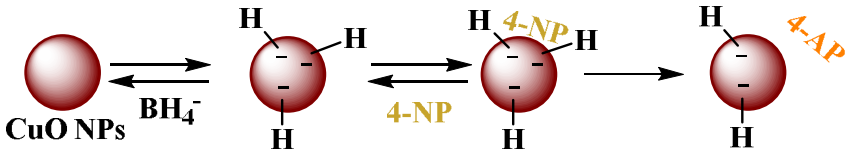

Figure 6: Scheme of the Langmuir–Hinshelwood mechanism for the reduction of 4-NP on the surface of the CuO nanoparticles.

As $NaBH_4$ was in excess compared to the 4-NP concentration, the reduction rates can be regarded as being independent of its concentration. Consequently, the reduction can be considered as a pseudo-first order reaction, and therefore, the correlation between $ln(C_t/C_0)$ and reaction time is linear (Figure 7). As the absorbance of 4-NP is proportional to its concentration in the medium, the ratio of A_t/A_0 is equivalent to the ratio of C_t/C_0 (A_t is the absorbance at time t, A_0 is the absorbance at time $t = 0$, C_t is the concentration of 4-NP at reaction time t and C_0 is the initial concentration of 4-NP). In this context, the apparent rate constant, k_{app}, was calculated from the slope in Figure 7. The values are summarized in Table 2, together with the rate constant normalized per mmol of metal content (k_n).

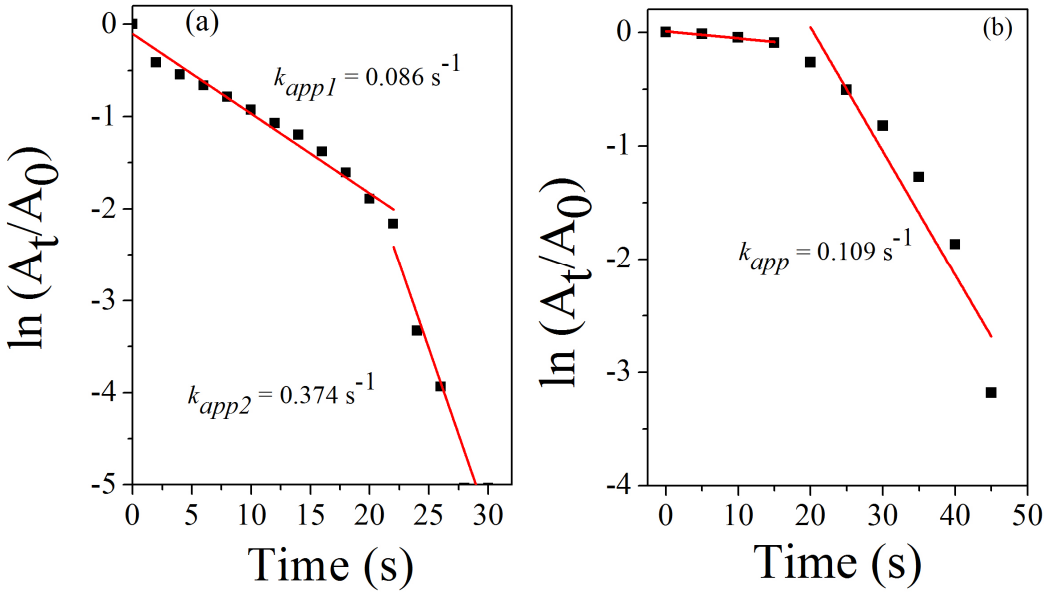

Figure 7. Pseudo-first order plots of 4-NP reduction with (a) Cu/MCM-41-10 and (b) Cu/MCM-41-24.

Table 2. Catalytic parameters for 4-NP reduction catalyzed by the Cu-MCM-41 catalysts.

Catalyst	t^a (s)	t_i^b (s)	$k_{app}{}^c$ (s^{-1})	$k_n{}^d$ (s^{-1}mmol^{-1})
Cu/MCM-41-10	30	0	0.086 (r^2 = 0.97)	409
			0.374 (r^2 = 0.92)	
Cu/MCM-41-24	50	15	0.109 (r^2 = 0.88)	13

[a] Reaction time to achieve maximum 4-NP conversion to 4-AP.
[b] Induction period.
[c] Determined from the slope of $\ln(A_t/A_0) = -kt$ plots.
[d] Calculated as $k_n = k_{app}$ (s^{-1})/n_{Cu} (mmol).

From Figure 7, it can be observed that upon addition of the Cu/MCM-41-10 catalyst, no induction time (t_i) is observed. The 4-NP reduction reaction started immediately upon the addition of the catalyst and two reaction rates profiles were observed, the first one exhibited a slower rate constant (0.086 s^{-1}, until 20 s of reaction) comparing with the second (0.374 s^{-1}). The lower reaction rate in the early stages of the

reaction could be due to competition between substrate reduction *vs* substrate/$NaBH_4$ adsorption on the catalyst surface.

Nonetheless, upon the addition of the Cu/MCM-41-24 catalyst, a period of induction time, t_i = 15 s, is required to start the reduction reaction. After that, the reaction becomes stationary, following a first-order rate law. From the latter linear part, the degradation rate constant (k_{app}) was calculated as 0.109 s^{-1}, better than that reported by Deka and co-workers using Cu-NPs (2.4×10^{-2} s^{-1}) [41]. The induction period shown in Figure 6b was also reported in catalysts based on Au NPs deposited over different supports, such as silica-coated manganese(II) ferrites [10] and spherical polyelectrolyte brushes consisting of poly([2-aminoethyl]- methacrylate hydrochloride) chains attached on polystyrene [42]. Other noble metal NPs [24,40] also shown this induction effect, and it is usually attributed to the diffusion time required for 4-NP to be adsorbed onto the catalyst's surface before starting the reaction. However, diffusion control can be definitely ruled out by mesoporous catalysts. Wunder *et al.*[42] suggested that this time can be assigned to a surface rearrangement, necessary to turn metal nanoparticles into an active catalyst. Moreover, Nemanashi *et al.* [43] assigned this period to the time needed for $NaBH_4$ to eliminate surface oxides.

In order to compare these results with the literature, a brief review on various CuO based catalysts for the reduction of 4-NP to 4-AP is presented in Table 3. Nasrollahzadeh *et al.* [44] synthesized CuO NPs by aqueous extraction of *Gundelia tournefortii* and obtained a reduction rate constant of 0.045 s^{-1} using similar conditions. Zhao *et al.* reported, in a review, rate values from 1.6×10^{-3} to 2.4×10^{-2} s^{-1} for Cu NP catalysts obtained by different methodologies [44]. The authors also point out that caution should be taken when using Cu NPs due to their high propensity for oxidation; thus, CuO NPs are, in fact, the responsible for the catalytic activity. Morales *et al.* [37]

achieved lower rate constants (0.299 s^{-1}) using Cu catalysts supported on high surface area graphite under the same reaction conditions.

Table 3. Comparison of rate constants (k_{app}) of different CuO catalysts for the reduction of 4-nitrophenol to 4-aminophenol.

Sample	Quantity (mg)	[$NaBH_4$] (mM)	[4-NP] (mM)	Rate Constant (k_{app}) (s^{-1})	Ref.
CuO NPs	10	250	2.5	45×10^{-3}	[48]
CuO hollow nanostructures	1	6.7	0.10	13×10^{-3}	[45]
CuO nanorods	1	100	6.00	6.7×10^{-3}	[46]
CuO NPs	2	8	0.12	2×10^{-3}	[47]
CuO nanosheets	0.3	20	0.10	35.5×10^{-3}	[48]

From a comparison of the rate constants reported in Table 3, it is worth noting that both materials prepared in this work present better catalytic activity, in terms of k_{app}, for the reduction of 4-NP. Actually, Cu/MCM-41-10 showed more than an eight-fold increase in the rate constant. This fact could be attributed to an effective dispersion of the CuO phase over the mesoporous support.

A better comparison between the catalytic activities of the catalysts can be performed by normalizing the k_{app} values to the amount of Cu on each catalyst (measured by AAS). Hence, a second constant (k_r) was determined. This value (see Table 3) is significantly higher for Cu/MCM-41-10 (409 $s^{-1}mmol^{-1}$) than for Cu/MCM-41-24 (13 $s^{-1}mmol^{-1}$) and highlights its better catalytic performance, albeit with a lower Cu loading. Comparing the calculated unit cell parameter (a_0) by XRD we can observe a higher disorder in the sample Cu/MCM-41-24, and this can be related to the lower catalytic activity in 4-NP reduction. On the other hand, this catalyst has CuO NPs of 15 nm, whereas in the sample Cu/MCM-41-10, it was not possible verify the diffraction of CuO NPs by XRD, although Cu is present by AAS and XPS analyses. This indicates a

very small size of the CuO particles, which present a more superficial area and hence higher catalytic active sites.

3.3. Catalyst recyclability

The reusability of heterogeneous catalysts is a great advantage for cost reduction of process chemistry, since it allows easiness of separation and recovery for practical catalytic applications. For this reason, the reusability was investigated by recovering the catalysts from the reaction mixture by filtration and testing them in a new reaction cycle without any prior treatment. As shown in Figure 8, both catalysts can be successfully recycled for ten consecutive runs without loss of activity, suggesting the high stability of the materials. In the case of Cu/MCM-41-10, the catalyst preserved the catalytic performance in terms of reaction time and 4-NP conversion. On the other hand, when Cu/MCM-41-24 was used, it can be seen that in the first cycle the conversion is lower after 30 s of reaction and then improves in the following cycles (Figure 8).

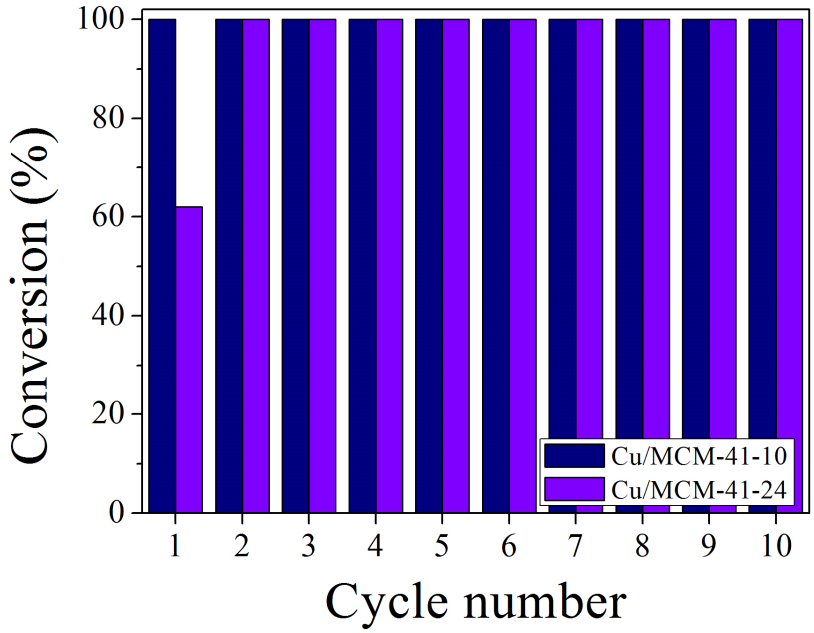

Figure 8. Recycling tests of Cu-MCM-41 catalysts. Conversions calculated after 30 s.

This result may suggest the disappearance of the induction time due to a rearrangement on the catalyst surface, as was mentioned above, and is accompanied by a color change in the solid after the first reaction.

After ten consecutive cycles, the Cu-catalysts were further characterized by FTIR spectra. The FTIR spectra of Cu/MCM-41-10 and Cu/MCM-41-24 after the recycling tests did not exhibit changes when compared to the FTIR spectra of the original catalysts (Figure 9), which confirms that the solid structure is preserved upon recycling and reuse.

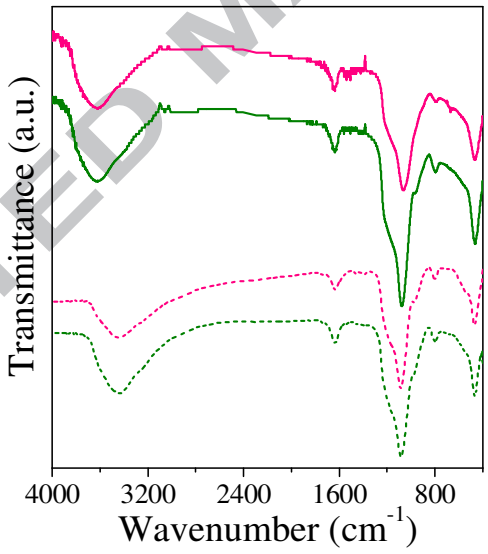

Figure 9. FTIR spectra of Cu/MCM-41-10 (pink) and Cu/MCM-41-24 (green). Solid line: before reaction, dash line: after reaction.

4. CONCLUSIONS

In this work it has been confirmed that the mesoporous silica MCM-41 support is very suitable for metal modification by a simple and reproducible procedure of wetness impregnation, which ensures a high metal content. The characterizations indicate that the mesoporous character is retained after metal loading.

Both catalysts obtained, Cu/MCM-41-10 and Cu/MCM-41-24, showed a high catalytic activity in the reduction of 4-NP to 4-AP (substrate conversion of ≈ 100%), with k_n values significantly higher for Cu/MCM-41-10 (409 $s^{-1}mmol^{-1}$) than for Cu/MCM-41-24 (13 $s^{-1}mmol^{-1}$). Furthermore, both catalysts could be reused in ten consecutives cycles, preserving or even increasing their catalytic performance, as in the case of Cu/MCM-41-24, retaining the original structure.

The use of a high surface area support enables the development of efficient and stable as noble metal catalysts. Regarding this fact, the replacement of precious metals, such as Pd, Au and Pt, for water pollutant remediation with non-precious metals, such as copper, is of significant economic importance as it can lead to less expensive and green methods for removing organic pollutants from contaminated sources.

Acknowledgements

This work was partially supported by Fundação para a Ciência e a Tecnologia (FCT)/MEC and FEDER under Program PT2020 project UID/QUI/50006/2013-POCI/01/0145/FEDER/007265 and UID/MULTI/00612/2013 (CQB), Portugal. M. Rocha thanks FCT for the grant SFRH/BD/52529/2014.

REFERENCES

[1] A.M. Tafesh, J. Weiguny, Chem. Rev. 96 (1996) 2035–2052.

[2] N. Sahiner, H. Ozay, O. Ozay, N. Aktas, Appl. Catal. B 101 (2010) 137–143.

[3] S. Saha, A. Pal, S. Kundu, S. Basu, T. Pal, Langmuir 26 (2010) 2885-2893.

[4] X. Guo, Z. Wang, S. Zhou, Talanta 64 (2004) 135–139.

[5] P. Mulchandani C.M. Hangarter, Y. Lei, W. Chen, A. Mulchandani, Biosens. Bioelectron. 21 (2005) 523–527.

[6] http://www.epa.gov/ttn/atw/hlthef/nitrophe.html

[7] S. Panigrahi, S. Basu, S. Praharaj, S. Pande, S. Jana, A. Pal, S.K. Ghosh, T. Pal, J. Phys. Chem. C 111 (2007) 4596-4605.

[8] S.C. Mitchell, R.H.Waring, Ullmann's Encyclopedia of Industrial Chemistry, Wiley-VCH, Weinheim, 2002.

[9] K. Kuroda, T. Ishida, M. Haruta, J. .Mol. Cat. A: Chem. 298 (2009) 7–11.

[10] M. Rocha, C. Fernandes, C. Pereira, S.L.H. Rebelo, M.F.R. Pereira, C. Freire, RSC Adv., 5 (2015) 5131–5141.

[11] H. Li, L. Han, J. Cooper-White, I. Kim, Green Chem.14 (2012) 586–591.

[12] S. Saha, A. Pal, S. Kundu, S. Basu, T. Pal, Langmuir 26 (2010) 2885–2893.

[13] Z. Jiang, J. Xie, D. Jiang, J. Jing, H. Qin, CrystEngComm 14 (2012) 4601–4611.

[14] A. Goyal, S. Bansal, S. Singhal, Inter. J. Hydrog. Energy 39 (2014) 4895-4908.

[15] J.M. Song, S.S. Zhang, S.H. Yu, Small 10 (2014) 717–724.

[16] R. Prucek, L. Kvítek, A. Panácek, L. Vancurová, J. Soukupová, D. Jancik, R. Zboril, J. Mater. Chem. 19 (2009) 8463-8469.

[17] A.K. Patra, A. Dutta, A. Bhaumik, Catal. Commun. 11 (2010) 651-655.

[18] T. R. Gundala, K. Godugu, N. C. G. Reddy, Adv. Synth. Catal. 360 (2018) 995-1006.

[19] M. Nasrollahzadeh, A. Ehsani, M. Maham, Synlett 25 (2014) 505-508.

[20] M. Nasrollahzadeh, A. Zahraei, A. Ehsani, M. Khalaj, RSC Adv. 4 (2014) 20351-20357.

[21] R. Xu, H. Bi, G. He, J. Zhu, H. Chen, Mater. Res. Bull. 57 (2014) 190–196.

[22] P. Zhang, Y. Sui, G. Xiao, Y. Wang, C. Wang, B. Liu, G. Zou, B. Zou, J. Mater. Chem. A1 (2013) 1632-1638.

[23] P. Deka, R.C. Deka, P. Bharali, New J. Chem. 38 (2014) 1789-1793.

[24] R. Bendi, R. Imae, RSC Adv. 3 (2013) 16279-16282.

[25] W.J. Liu, K. Tian, H. Jiang, H.Q. Yu, Green Chem. 16 (2014) 4198–4205.

[26] V. Narayanan, Mater. Res. 11 (2008) 443-446.

[27] N. Wei, X. Zou, H. Huang, X. Wang, W. Ding, X. Lu, Eur. J. Org. Chem. 2 (2018) 209–214.

[28] M.T. Bore, M.P. Mokhonoana, T.L. Ward, N.J. Coville, A.K. Datye, Microporous Mesoporous Mater. 95 (2006) 118-125.

[29] J.S. Beck, J.C. Vartuli, W.J. Roth, M.E. Leonowicz, C.T. Kresge, K.D. Schmitt, C. T-W. Chu, D.H. Olson, E.W. Sheppard, S.B. McCullen, J.B. Higgins, J.L. Schlenkert, J. Am. Chem. Soc. 1992, 114, 10834-10843.

[30] Y. Han, L. Zhao, J. Y. Ying, Adv. Mater 19 (2007) 2454-2459.

[31] P. Fu, T. Yang, J. Feng, H. Yang, J. Ind. Eng. Chem. 29 (2015) 338-343.

[32] S. K. Das, P. Deka, M. Chetia, R. C. Deka, P. Bharali, U. Bora, Catal. Lett. 148 (2018) 547-554.

[33] D. Rath, K. M. Parida, Ind. Eng. Chem. Res. 50 (5) (2011) 2839-2849.

[34] G.A. Eimer, L.B. Pierella, G.A. Monti, O.A. Anunziata, Catal. Lett. 78 (2002) 65-74.

[35] S.S. Bhoware, A.P. Singh, J. Mol. Catal. A: Chem. 266 (2007) 118-130.

[36] X. Ma, H. Chi, H. Yue, Y. Zhao, Y. Xu, J. Lv, S. Wang, J. Gong, AIChE J. 59 (2013) 2530-2539.

[37] M.V. Morales, M. Rocha, C. Freire, E. Asedegbega-Nieto, E. Gallegos-Suarez, I. Rodríguez-Ramos, A. Guerrero-Ruiz, Carbon 111 (2017) 150-161.

[38] Z. Yan, L. Fu, X. Zuo, H. Yang, Appl. Catal. B: Environ. 226 (2018) 23-30.

[39] P. Zhao, X. Feng, D. Huang, G. Yang, D. Astruc, Coord. Chem. Rev. 287 (2015) 114-136.

[40] P. Hervés, M. Pérez-Lorenzo, L. M. Liz-Marzán, J. Dzubiella, Y. Lub, M. Ballauff, Chem. Soc. Rev. 41 (2012) 5577–5587.

[41] P. Deka, R.C. Deka, P. Bharali, New J. Chem. 38 (2014) 1789-1793.

[42] S. Wunder, Y. Lu, M. Albrecht, M. Ballauff, ACS Catal. 1 (2011) 908-916.

[43] M. Nemanashi, R. Meijboom, J. Colloid. Interface Sci. 389 (2013) 260-267.

[44] M. Nasrollahzadeha, M. Maham, S.M. Sajadi, J. Colloid Interface Sci. 455 (2015) 245–253.

[45] I. Singh, K. Landfester, A. Chandra, R. Muñoz-Espí, Nanoscale 7 (2015) 19250–19258.

[46] A. Bhattacharjee, M. Ahmaruzzaman, RSC Adv. 6 (2016) 41348–41363.

[47] A. Sharma, R.K. Dutta, A. Roychowdhury, D. Das, A. Goyal, A. Kapoor, Appl. Catal., A, 543 (2017) 257–265.

[48] W. Che, Y. Ni, Y. Zhang,Y. Ma, J. Phys. Chem. Solids, 77 (2015) 1–7.

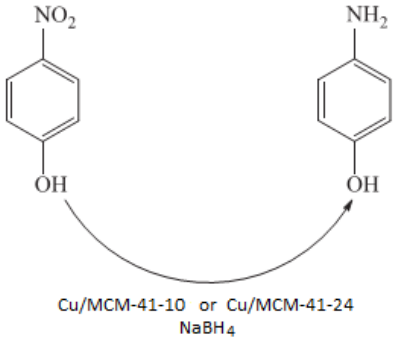

Graphical abstract

Synopsis:

Copper-mesoporous-based catalysts were prepared by impregnation of MCM-41 with copper acetylacetonate. The Cu-based catalysts led to almost 100% reduction of 4-nitrophenol to 4-aminophenol in aqueous medium in 30 and 50 sec, for Cu/MCM-41-10 and Cu/MCM-41-24, respectively. Both catalysts were stable and reusable up to ten times in consecutive runs.